Gene therapy rescues photoreceptor blindness in dogs and paves the way for treating human X-linked retinitis pigmentosa

William A. Beltran[a,1], Artur V. Cideciyan[b], Alfred S. Lewin[c], Simone Iwabe[a], Hemant Khanna[d,e], Alexander Sumaroka[b], Vince A. Chiodo[f], Diego S. Fajardo[c], Alejandro J. Román[b], Wen-Tao Deng[f], Malgorzata Swider[b], Tomas S. Alemán[b], Sanford L. Boye[f], Sem Genini[a], Anand Swaroop[d,g], William W. Hauswirth[f], Samuel G. Jacobson[b], and Gustavo D. Aguirre[a,1]

[a]Section of Ophthalmology, School of Veterinary Medicine, University of Pennsylvania, Philadelphia, PA 19104; [b]Department of Ophthalmology, Scheie Eye Institute, University of Pennsylvania Perelman School of Medicine, Philadelphia, PA 19104; [c]Department of Molecular Genetics and Microbiology, University of Florida, Gainesville, FL 32610; [d]Department of Ophthalmology and Visual Sciences, University of Michigan, Ann Arbor, MI 48105; [e]Department of Ophthalmology, University of Massachusetts Medical School, Worcester, MA 01605; [f]Department of Ophthalmology, University of Florida, Gainesville, FL 32610; and [g]Neurobiology-Neurodegeneration and Repair Laboratory, National Eye Institute, National Institutes of Health, Bethesda, MD 20892

Hereditary retinal blindness is caused by mutations in genes expressed in photoreceptors or retinal pigment epithelium. Gene therapy in mouse and dog models of a primary retinal pigment epithelium disease has already been translated to human clinical trials with encouraging results. Treatment for common primary photoreceptor blindness, however, has not yet moved from proof of concept to the clinic. We evaluated gene augmentation therapy in two blinding canine photoreceptor diseases that model the common X-linked form of retinitis pigmentosa caused by mutations in the retinitis pigmentosa GTPase regulator (RPGR) gene, which encodes a photoreceptor ciliary protein, and provide evidence that the therapy is effective. After subretinal injections of adeno-associated virus-2/5–vectored human RPGR with human IRBP or GRK1 promoters, in vivo imaging showed preserved photoreceptor nuclei and inner/outer segments that were limited to treated areas. Both rod and cone photoreceptor function were greater in treated (three of four) than in control eyes. Histopathology indicated normal photoreceptor structure and reversal of opsin mislocalization in treated areas expressing human RPGR protein in rods and cones. Postreceptoral remodeling was also corrected: there was reversal of bipolar cell dendrite retraction evident with bipolar cell markers and preservation of outer plexiform layer thickness. Efficacy of gene therapy in these large animal models of X-linked retinitis pigmentosa provides a path for translation to human treatment.

retina | retinal degeneration

Photoreceptors function cooperatively with the retinal pigment epithelium (RPE) to optimize photon catch and generate signals that are transmitted to higher vision centers and perceived as a visual image. Disruption of the visual process in the retinal photoreceptors can result in blindness. Genetic defects in the retina cause substantial numbers of sight-impairing disorders by a multitude of mechanisms (1, 2). These genetic diseases were classically considered incurable, but the past few years have witnessed a new era of retinal therapeutics in which successful gene therapy of an animal model of one blinding human disease (3) was followed by stepwise translation to the clinic. The RPE65 form of Leber congenital amaurosis, due to a biochemical blockade of the retinoid cycle in the RPE, was the first and remains the only blinding genetic disease to be successfully treated in humans (reviewed in ref. 4).

The next level of challenge is to initiate treatment for the majority of blinding retinal disorders in which the genetic flaws are primarily in the photoreceptors. Successful targeting of therapeutic vectors to mutant photoreceptors would be required to restore function and preserve structure. Among photoreceptor dystrophies, the X-linked forms of retinitis pigmentosa (XLRP) are one of the most common causes of severe vision loss (5). More than 25 y ago, the genetic loci were identified (6), and discovery of the underlying gene defects followed (7, 8). Mutations in the retinitis pigmentosa GTPase regulator (RPGR) gene account for >70% of the cases of XLRP (9–11), and exon ORF15, a mutational hot spot in RPGR, is mutated in 22–60% of patients (12, 13). Males affected with RPGR-XLRP typically have night blindness in their first decade of life followed by reduction of their visual field and loss of visual acuity. By the end of their fourth decade, most patients are legally blind (14–16).

Disease-relevant animal models have been crucial in developing and validating new therapies. For RPGR-XLRP, there are both mouse (17–19) and canine models (20). In the dog, two naturally occurring distinct microdeletions in ORF15 result in different disease phenotypes. X-linked progressive retinal atrophy 1 [XLPRA1; deletion (del) 1,028–1,032] has a C-terminal truncation of 230 residues; the disease is juvenile, but postdevelopmental, in onset, and progresses over several years (20, 21). In contrast, the two-nucleotide deletion associated with XLPRA2 (del 1,084–1,085) causes a frameshift with inclusion of 34 basic amino acids that changes the isoelectric point of the putative protein, and truncation of the terminal 161 residues. The disease is early onset and rapidly progressive (20, 22). Both models correspond to the disease spectrum of human XLRP (5), and, although differing in relative severity, they would be equivalent to human disease occurring within the first decade of life (23).

In the present study, we used an adeno-associated virus (AAV) 2/5 vector-mediated transfer and found that gene augmentation in both rods and cones with the full-length human RPGRORF15 cDNA driven by the human IRBP promoter, and, to a lesser extent by the human G-protein–coupled receptor protein kinase 1 (hGRK1) promoter, prevented photoreceptor degeneration in both canine diseases and preserved retinal structure and function.

Results

RPGR ORF15 Mutations Lead to Photoreceptor Degeneration in Humans and Dogs.
Topography of photoreceptors can be mapped across the retina of patients with RPGR-XLRP by measuring

the thickness of the outer (photoreceptor) nuclear layer (ONL) using cross-sectional optical coherence tomography (OCT) retinal imaging (Fig. 1*A*). In normal eyes (*Inset*), ONL thickness peaks centrally and declines with distance from the fovea (24). XLRP patients with ORF15 mutations can have different disease patterns. A common pattern shows dramatic photoreceptor losses with relatively greater retention of ONL thickness at and near the cone-rich foveal region surrounded by a zone of detectable but markedly thinned ONL (Fig. 1*A*, P1). *RPGR* disease expression also includes the less common phenotype characterized by loss of central photoreceptors and diseased, yet better-preserved, peripheral photoreceptors (Fig. 1*A*, P2). The present examples, taken together with previous observations (16, 25–30), demonstrate that there can be a spectrum of human *RPGR*-XLRP phenotypes. Most of the phenotypes have more rod than cone dysfunction as measured by electroretinograms (ERGs) (30).

The two canine models can also be studied with cross-sectional retinal imaging, such as we use for human patients, and topographical photoreceptor maps can be generated and compared with normal data (Fig. 1*B*). Of translational importance is the fact that a spectrum of disease patterns also occurs in the canine models. XLPRA1 dogs, for example, can show ONL thinning with relative preservation of a region immediately superior to the optic nerve, corresponding to the high photoreceptor density of the visual streak (31). In contrast, an example of an XLPRA2 photoreceptor map shows a pattern of retina-wide ONL thinning, but more pronounced losses in the central retina, corresponding to the visual streak, than in the peripheral retina.

The natural history of photoreceptor degeneration was determined to select the age and retinal site for treatment in XLPRA1 and XLPRA2 (Fig. 1*C*). Spatiotemporal distribution of photoreceptor degeneration and the disease course were determined by quantifying ONL thickness along the vertical meridian (Fig. 1*C*). Wild-type dogs (WT) (*n* = 5, ages 7–43 wk) show a relatively uniform ONL thickness with slightly higher values (averaging 57 µm) superior to the optic nerve up to eccentricities of 35° and slightly lower values (averaging 54 µm) inferior to the optic nerve up to 25°. XLPRA1 at younger ages (*n* = 7, ages 7–28 wk) shows ONL thickness that is within or near normal limits (Fig. 1*C*). XLPRA1 at older ages (*n* = 6, ages 56–76 wk) shows ONL thinning in the inferior retina and relative preservation of the visual streak region immediately superior to the optic nerve (Fig. 1*C*, brackets). There can be greater differences among older XLPRA1 eyes, with some results near the lower limit of normal and others showing substantial ONL loss below 50% of WT (Fig. 1*C*), consistent with variable severity of disease as reported (21).

In XLPRA2 at the youngest ages examined (*n* = 2, ages 8 and 22 wk), we observed retina-wide ONL thinning that tended to be greater in the central retina (44% of WT), corresponding to the visual streak, than in the periphery (60% of WT) (Fig. 1*C*). Older XLPRA2 dogs (*n* = 3, ages 36–59 wk) show more ONL thinning with a tendency for greater central and inferior retinal disease (30% of WT) than in the superior peripheral retina (45% of WT) (Fig. 1*C*). ONL thickness in the oldest XLPRA1 and XLPRA2 eyes was substantially reduced (Fig. 1*C*).

Rod and cone retinal function in young and older dogs with XLPRA1 and XLPRA2 was measured by ERG (32). Both XLPRA1 and XLPRA2 diseases could be characterized as having more rod than cone dysfunction. Younger XLPRA1 eyes (*n* = 6) showed abnormal (4/6) rod function but normal cone function (Fig. 1*D*) whereas older XLPRA1 eyes (*n* = 7) showed abnormal rods (6/7) and cones (5/7) (Fig. 1*D*). Younger XLPRA2 eyes (*n* = 3) had abnormal rod function but mostly (2/3) normal cone function, but older XLPRA2 eyes (*n* = 6) had abnormal rod and cone function (Fig. 1*D*). Defining the differences in the structural and functional natural history of XLPRA1 and XLPRA2 diseases showed a sufficient overlap in the noninvasive studies in dogs and humans to validate the use of the dog models in proof-of-concept studies of treatment that may be relevant to *RPGR*-XLRP patients.

Treatment of XLPRA with Gene Augmentation Therapy: In Vivo Findings. Subretinal injection of the full-length human *RPGR*ORF15 cDNA under control of the hIRBP (*AAV2/5-hIRBP-hRPGR*)

promoter was performed in both XLRPA1 and XLPRA2 and under control of the hGRK1 (*AAV2/5-hGRK1-hRPGR*) promoter in XLPRA2 (Table S1). In XLPRA1, treatment was initiated at 28 wk, before photoreceptor loss, and monitored to 77 wk, well after the start of degeneration (21) (Fig. 1*C*). In XLPRA2, the injections were performed at 5 wk of age, and the study terminated at 38 wk. These experiments were preceded by a series of studies with absence of rescue and some with complications (Table S2). In contrast to these treatment failures, the full-length
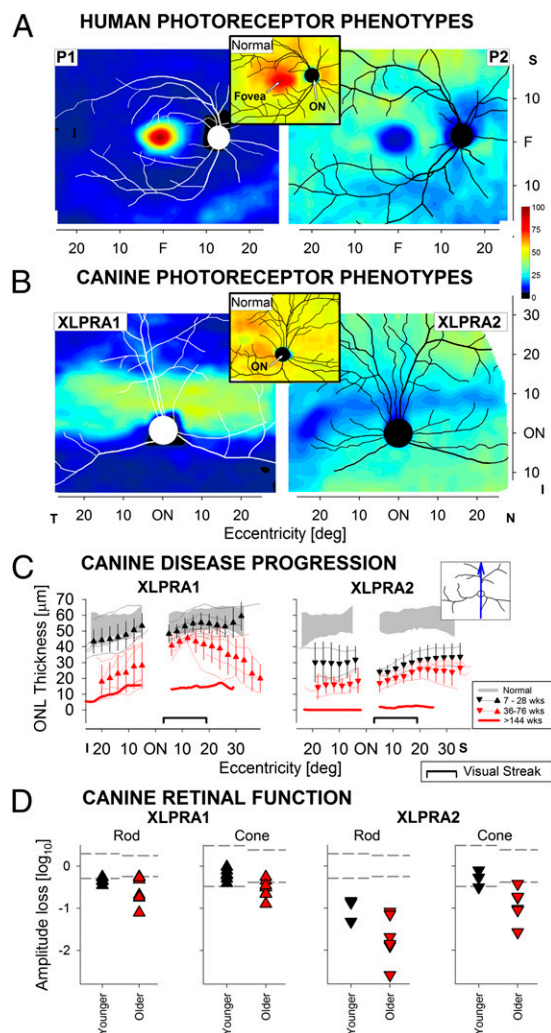

Fig. 1. Retinal disease phenotypes caused by *RPGR*ORF15 mutations in human patients and in dogs. (*A*) Different patterns of photoreceptor topography in two XLRP patients with *RPGR* mutations (P1: c.ORF15+483_484delGA, p.E746fs; P2: c.ORF15+ 652_653delAG, p.E802fs). ONL thickness topography is mapped to a pseudocolor scale. (*Inset*) Representative normal subject. Location of fovea and optic nerve (ON) are shown. (*B*) Different patterns of photoreceptor topography in the canine models of *RPGR*ORF15; mapping as performed with the human data. (*Inset*) Map of a representative WT dog with location of ON labeled. (*C*) ONL thickness profile along the vertical meridian (*Inset*) comparing XLPRA1 and XLPRA2 of different ages (thin traces) versus normal results (gray band). Mean (±SD) results are from groups of younger (7–28 wk) and older (36–76 wk) dogs. The thicker red line represents the data from the oldest dogs examined (>144 wk old). Brackets mark the location of the high photoreceptor density corresponding to the canine visual streak. (*D*) Rod and cone retinal function by ERGs in XLPRA1 (young: 7–23 wk; old: 56–80 wk) and XLPRA2 (young: 8–22 wk; old: 38–144 wk) dogs shown as the logarithm of amplitude loss from the mean WT value (rod: 2.39 and 2.38 log₁₀ µV and cone: 1.50 and 1.72 log₁₀ µV for younger and older, respectively). Each symbol represents an eye. Horizontal dashed lines represent the WT limits (±2 SD).
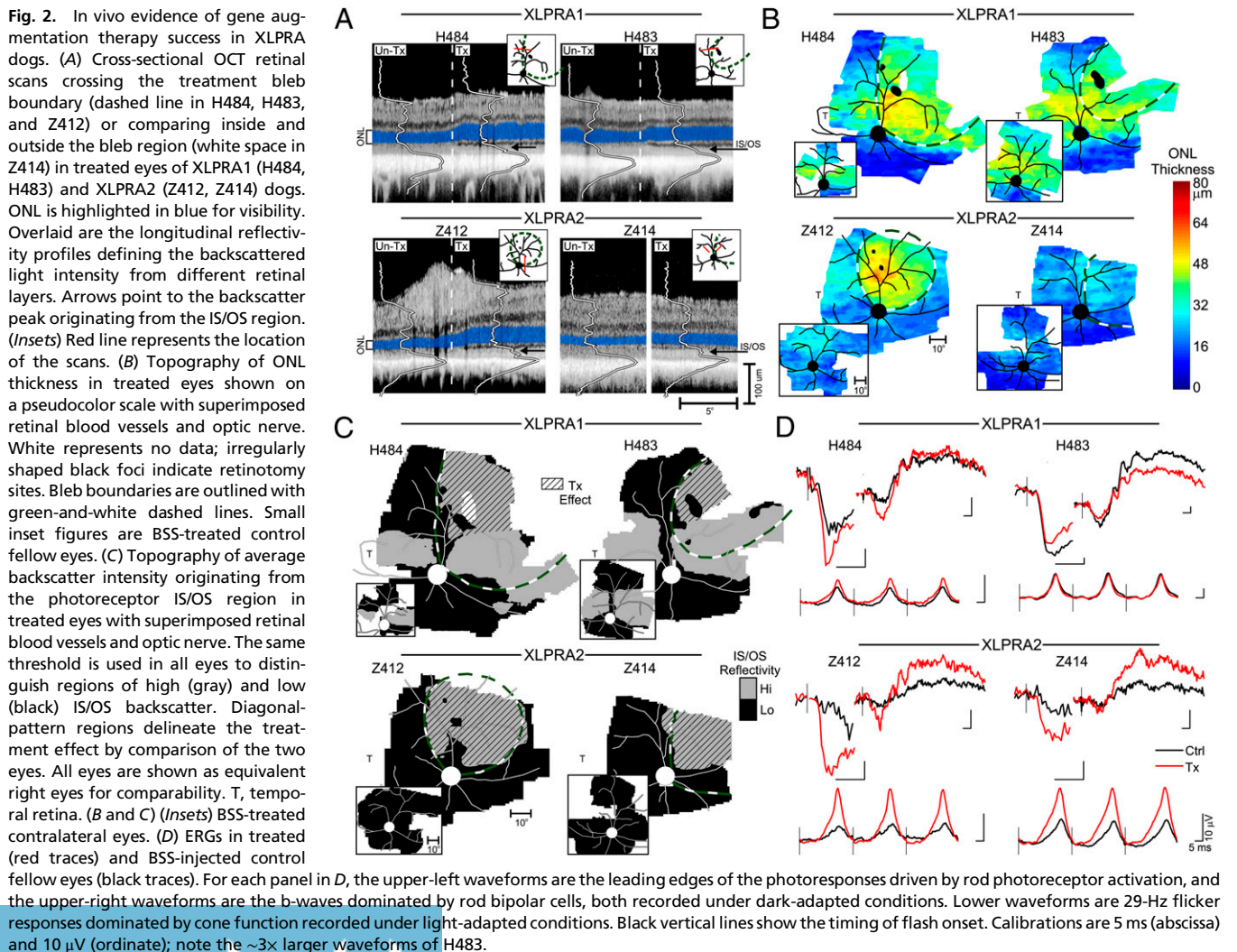
Beltran et al.

human *RPGR*ORF15 (driven by hIRBP or hGRK1 promoters) was therapeutically effective.

The positive treatment response was detectable in vivo. Treated eyes of XLPRA1 dogs had thicker ONL in the superior peripheral retina, specifically on the treated side of the subretinal injection area (bleb) boundary compared with the untreated side (Fig. 2*A*). In addition, the signal peak corresponding to the region of the photoreceptor inner and outer segments (IS/OS) was more intense and better organized on the treated side (Fig. 2*A*). Treated eyes of XLPRA2 dogs showed thicker ONL on the treated side or higher intensity signal at the level of the IS/OS (Fig. 2*A*). To understand better the relationship between the treatment bleb and local retinal structure, ONL thickness was mapped across wide expanses of the treated and control eyes (Fig. 2*B*). XLPRA1 dog H484 at 76 wk of age had a clearly demarcated zone of ONL retention within the treatment bleb in superior peripheral retina (Fig. 2*B*). There was ONL degeneration outside the bleb in the superior temporal retina. In the central retinal region where XLPRA1 dogs at this age retain near normal ONL thickness (Fig. 1*C*), a transition across the bleb boundary was less detectable (Fig. 2*B*).

XLPRA1 dog H483 with a smaller subretinal bleb had similar findings in the superior peripheral region with local evidence of ONL thickness retention inside the bleb boundary. More centrally, both treated and untreated regions retained near normal ONL thickness, and there was no change in ONL thickness corresponding to the bleb boundary (Fig. 2*B*). XLPRA2 dog

Z412 showed a region with preserved ONL that corresponded to the bleb boundary; ONL was abnormally thinned outside this boundary (Fig. 2*B*). Longitudinal follow-up from 21 to 36 wk showed the time course of ONL degeneration outside the bleb of the treated eye and in the balanced salt solution (BSS)-injected control eye (Fig. S1). XLPRA2 dog Z414 showed a region of slight ONL thickness retention approximately corresponding to the bleb boundary (Fig. 2*B*).

Changes at the level of photoreceptor IS/OS were quantified. Backscatter intensity at this layer was segmented and mapped (Fig. 2*C*). IS/OS intensity maps of three of the treated dogs (H484, H483, and Z412) were similar to the ONL maps, such that regions of retained ONL corresponded to higher intensity. In the case of Z414, the treated region showed substantially higher backscatter intensity at the IS/OS layer, and this was consistent with the better layer definition apparent in individual scans (Fig. 2*A*). Comparison of the treated and BSS-injected control eyes showed the clearly delineated retinal regions with treatment-related effects (Fig. 2*C*, diagonal pattern). ERGs were evaluated in terms of interocular asymmetry (Fig. 2*D*). Signals were larger in the treated eyes of three dogs (H484, Z412, and Z414) for photoreceptor responses dominated by rods and for postreceptoral bipolar cell responses mediated by both rods and cones. H483 had the least degenerate retina and normal amplitude responses bilaterally (Fig. 2*D* and Fig. S2) that were symmetric for cones and asymmetric for rods, favoring the untreated eye.

Fig. 2. In vivo evidence of gene augmentation therapy success in XLPRA dogs. (*A*) Cross-sectional OCT retinal scans crossing the treatment bleb boundary (dashed line in H484, H483, and Z412) or comparing inside and outside the bleb region (white space in Z414) in treated eyes of XLPRA1 (H484, H483) and XLPRA2 (Z412, Z414) dogs. ONL is highlighted in blue for visibility. Overlaid are the longitudinal reflectivity profiles defining the backscattered light intensity from different retinal layers. Arrows point to the backscatter peak originating from the IS/OS region. (*Insets*) Red line represents the location of the scans. (*B*) Topography of ONL thickness in treated eyes shown on a pseudocolor scale with superimposed retinal blood vessels and optic nerve. White represents no data; irregularly shaped black foci indicate retinotomy sites. Bleb boundaries are outlined with green-and-white dashed lines. Small inset figures are BSS-treated control fellow eyes. (*C*) Topography of average backscatter intensity originating from the photoreceptor IS/OS region in treated eyes with superimposed retinal blood vessels and optic nerve. The same threshold is used in all eyes to distinguish regions of high (gray) and low (black) IS/OS backscatter. Diagonal-pattern regions delineate the treatment effect by comparison of the two eyes. All eyes are shown as equivalent right eyes for comparability. T, temporal retina. (*B* and *C*) (*Insets*) BSS-treated contralateral eyes. (*D*) ERGs in treated (red traces) and BSS-injected control fellow eyes (black traces). For each panel in *D*, the upper-left waveforms are the leading edges of the photoresponses driven by rod photoreceptor activation, and the upper-right waveforms are the b-waves dominated by rod bipolar cells, both recorded under dark-adapted conditions. Lower waveforms are 29-Hz flicker responses dominated by cone function recorded under light-adapted conditions. Black vertical lines show the timing of flash onset. Calibrations are 5 ms (abscissa) and 10 μV (ordinate); note the ~3× larger waveforms of H483.

Gene Augmentation Rescues Photoreceptors and Reverses Mislocalization of Rod and Cone Opsins in Both XLPRA Genotypes. Assessment of retinal morphology in tissue sections that included the bleb boundary confirmed the in vivo imaging results of retention of ONL thickness and photoreceptor preservation in subretinally-treated areas (Fig. 3, panels 1–5; Fig. S3). Intravitreal vector administration was comparable to no treatment (Table S1). In the three dogs treated with *AAV2/5-hIRBP-hRPGR* (H484, H483, Z412), rod and cone IS and OS structure was normal within the bleb boundary. In the untreated areas, IS were short and OS were sparse and irregular (Fig. 3, panels 3 and 4; Fig. S3). In Z414, treated with *AAV2/5-hGRK1-hRPGR*, a milder yet positive photoreceptor rescue was observed in the bleb area (Fig. S3C). Immunolabeling with an antibody directed against human RPGRORF15 (33) detected robust hRPGR protein expression limited to photoreceptors in the treatment area (Table S1). Labeling was found throughout the IS and synaptic terminals in the four dogs, as well as in the rod and cone perinuclear region of H484 (Fig. 3, panels 6–8; Fig. S3). Finally, the mislocalization of rod and cone opsins, a feature of the disease in human (34), mouse (17), and dog (22, 35), was reversed (Fig. 3, panels 9, 10, 12, and 13; Fig. S3) in the three dogs treated with *AAV2/5-hIRBP-hRPGR*. Reduced yet distinct rod and red/green (R/G) cone opsin mislocalization was apparent in Z414 treated with *AAV2/5-hGRK1-hRPGR* (Fig. S3C).
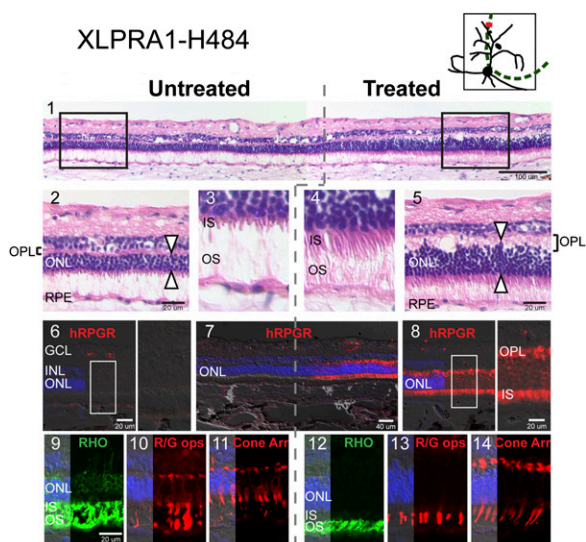
Prevention of Secondary OPL, Bipolar Cell, and Inner Retinal Disease. In XLPRA, as in other primary photoreceptor diseases, OPL and inner retinal abnormalities are common secondary effects (22, 35–37). In untreated regions, narrowing of the OPL was associated with compressed photoreceptor synaptic terminals (Fig. 3, panels 2 and 5; Fig. S3) and with a reduction of the number of CtBP2-labeled synaptic ribbons in rod and cone terminals (Fig. 4, panels 1 and 2; Fig. S4). In parallel, rod and cone bipolar cell dendrites retracted (Fig. 4, panels 3 and 4; Fig. S4). These secondary changes were absent in treated areas, resulting in a preserved OPL. In contrast, calbindin labeling of horizontal and amacrine cells (Fig. 4, panels 5 and 6; Fig. S4) and their lateral processes was normal and unchanged between treated and untreated regions. These last-mentioned hallmarks, however, are of late-stage retinal remodeling in XLPRA (22, 35) and were not expected to be present at the age when dogs were terminated.

The dendritic terminals of horizontal cells, as well as those of ganglion cells, and the nerve fiber layer of treated and untreated regions appeared normal when labeled with an antibody directed against the neurofilament heavy chain (NF200 kDa). However, there was punctate NF200 staining in the ONL. Overexpression of neurofilaments is a characteristic of axonal injury in several neurodegenerative disorders and occurs in this and other retinal diseases (38). This finding was restricted to the untreated regions of all dogs and was absent or reduced in treated areas (Fig. 4, panels 5 and 6; Fig. S4). GFAP immunolabeling clearly delineated untreated regions that showed increased Müller glia reactivity, whereas labeling diminished in the transition zone between treated and untreated regions and was absent in the bleb area (Fig. 4, panels 7 and 8; Fig. S4). In summary, inner retinal rescue was complete in three of four treated eyes; rescue
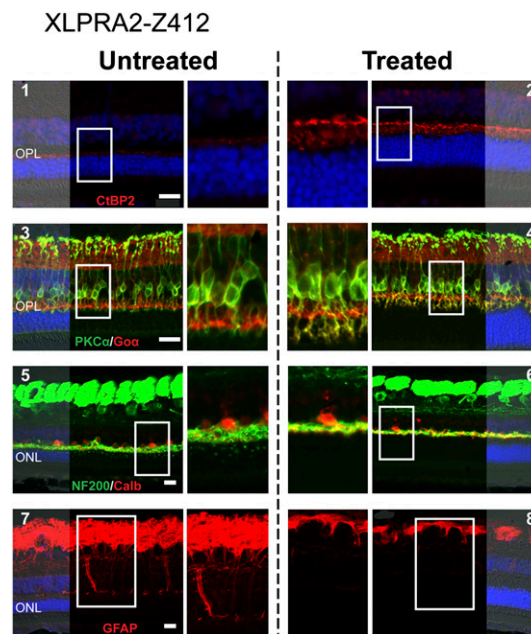

Fig. 3. Gene augmentation therapy rescues photoreceptors in the XLPRA1 dog H484 treated with *AAV2/5-hIRBP-hRPGR* at 28 wk of age and terminated at 77 wk. The schematic drawing illustrates the treatment area (dashed green lines) and the location of the region (red line) illustrated in the section. (1) Representative H&E-stained cryosection at the nontreated/treated junction (vertical dashed line). Boxed areas are illustrated at higher magnification below (2–5). Photoreceptor density is decreased in nontreated region and both ONL (white arrowheads) and OPL are narrowed; rod and cone IS are short, and OS sparse. In treated regions, the number of photoreceptors is increased and their structure is normal (4 and 5), resulting in thicker ONL and preserved OPL. (6–8) Expression of hRPGRORF15 in treated areas decreases in the transition zone and is absent elsewhere. Protein is present in rod and cone inner segments and synaptic regions and, to a lesser extent, in the perinuclear cytoplasm where expression is most intense. (9,10,12, and 13) Rod (RHO) and red/green cone (R/G ops) opsins are mislocalized in untreated regions with label in the IS, ONL, and synaptic terminals. Treated areas show normal localization to the OS. (11 and 14) Preservation of normal cone structure in treated areas is clearly shown with cone arrestin (Cone Arr) labeling. GCL, ganglion cell layer; INL, inner nuclear layer; IS, inner segments; ONL, outer nuclear layer; OPL, outer plexiform layer; OS, outer segments; RPE, retinal pigment epithelium.

Fig. 4. Successful gene therapy rescues retinal remodeling in the XLPRA2 dog Z412 treated with *AAV2/5-hIRPB-hRPGR* at 5 wk of age and terminated at 38 wk. Immunolabeling with CtBP2/RIBEYE shows a reduced number of photoreceptor synaptic ribbons in the untreated areas (1). In treated areas, the density of synaptic ribbons is normal, thus contributing to the preservation of the OPL thickness (2). Coimmunolabeling of rod bipolar (PKCα) and ON bipolar cells (Goα) shows retraction of dendrites in untreated areas (3), whereas dendritic arborization is preserved in treated regions (4). (5 and 6) Coimmunolabeling of the inner retina with antibodies to neurofilament 200 kDa (NF200) and calbindin (Calb) is normal in both untreated and treated regions, but punctate NF200 staining is seen in the ONL in untreated areas. (7 and 8) GFAP immunolabeling of Müller cell radial extensions is found only in untreated areas, whereas no reactive Müller cells are seen in the treated regions.

was partial for the eye treated with *AAV2/5-hGRK1-hRPGR* where rod neurite sprouting extended into the inner retina (Table S1), and the NF200 labeling pattern was intermediate between normal and disease (Fig. S4*C*). The results clearly show that targeting *RPGR* augmentation to photoreceptors in both XLPRA1 and XLPRA2 corrects the primary photoreceptor defect and has beneficial downstream effects as OPL and inner retinal abnormalities are prevented or reversed.

Discussion

Recent successes using gene replacement to treat LCA2, the autosomal recessive RPE disease due to *RPE65* mutations, have paved the way for considering gene therapy for treating other incurable human retinopathies (reviewed in refs. 4 and 39). XLRP is among the candidate diseases for treatment because it can be identified in the clinic through pedigree analysis, carrier identification, or by the fact that there is a high frequency of XLRP among simplex males with retinitis pigmentosa (13), and mutations in *RPGR*ORF15 account for about 75% of XLRP patients (40). The current results showing treatment efficacy in two large animal models of human *RPGR*ORF15-XLRP strongly suggest that a gene augmentation strategy is a viable option for this photoreceptor ciliopathy and complements successful rod rescue in a murine model of the Bardet–Biedl syndrome ciliopathy (41).

The disease in humans and in animal models is not, however, without complexity, and future therapy of the human disease will need to be approached with caution. For example, there are modifiers that may affect disease expression in both patients and dog models (30, 42), and there is a spectrum of phenotypes between and within *RPGR*-XLRP families (28) and in the dog XLPRA1 model (21). The phenotypic diversity may be a potential obstacle to patient selection and also points to the need for more than a molecular diagnosis and the patient's age as criteria to determine candidacy for treatment. In support of genotype data, there must be complementing, detailed, noninvasive retinal imaging and function studies. The temptation should be resisted in early human treatment approaches to try to design a treatment to fit all phenotypes and all disease stages. The dog diseases are mainly rod > cone degenerations, and there was efficacy in treating both the severe XLPRA2 with central retinal degeneration and the less severe XLPRA1 with central retinal preservation using vectors that targeted both rods and cones. Not included in the canine disease spectrum, however, are certain human *RPGR*-XLRP phenotypes, such as mild cone > rod or cone dystrophies (25, 26, 43–45). Some patients can show very limited or even normal rod function, and cone-targeting strategies must be developed for these subtypes. Proof-of-principle studies targeting cone diseases already have been successful in both mouse and dog models with mutations in cone photo-transduction (46) or cyclic GMP gated channel (47–49) genes, allowing translation to the clinic to be expedited.

The reported intrafamilial variation of phenotypes (28) neither excludes nor includes entire pedigrees from participation, but further strengthens the case for complete clarification of phenotype in individual patients. Furthermore, in the present study, there was no attempt to target the very central retina; the extracentral subretinal approach as used in the dogs would be the advisable strategy for early phase human clinical trials on the basis of the current observations. However, many *RPGR* patients show continued survival of foveal cones and impaired but useful visual acuity in late disease stages (15). Because subfoveal injections of viral vector constructs have been shown to cause loss of diseased foveal cones (50), an alternate means of therapeutic gene delivery should be considered. Advances in intravitreal delivery systems to treat the outer retina, for example, using mutant AAV capsid vectors (51), eventually could allay the safety concerns in treating residual foveal cones.

Although it is clear that *RPGR*-associated disease is common and generally severe, the function of the gene, and the association between mutation and disease, are less well understood. *RPGR* has a complex splicing pattern with multiple tissue- and cell-specific isoforms (52), is known to interact with a number of ciliary proteins (53, 54), acts as a guanine nucleotide exchange factor for small GTPase RAB8A (55), and may have a role in vertebrate development (56). Such complexity may account partially for the variability in disease phenotype. In general, loss-of-function (13, 17) or gain-of-function (19, 20, 22) mechanisms have been proposed (56), suggesting that each would require different therapeutic approaches. Although our present studies cannot rule out either mechanism as causal to disease, the results clearly indicate that gene augmentation alone is effective in preventing disease or in arresting and reversing the degenerative process in canine models of ORF15 mutations. These fundamental findings allow us to move forward therapeutically toward translational studies while the specific disease mechanisms await further elucidation.

Our results emphasize that targeting therapy to rod and cone photoreceptors is essential for functional and structural rescue in *RPGR*-associated retinal disease. The hIRBP promoter that regulates expression of the therapeutic gene results in robust expression of reporter or therapeutic genes in both cell types (Fig. S5; Fig. 3, panels 6–8; Fig. S3), and expression is sustained. As IRBP also is expressed in human cones (57), we expect efficient targeting of rods and cones with this promoter in future translational studies. When regulated by the hGRK1 promoter, the therapeutic transgene expression was low in rods and, to a lesser extent, in cones. The remaining photoreceptor structure, albeit abnormal, was considerably improved over untreated regions.

In XLPRA1, treatment before disease onset prevented disease development. Furthermore, treatment of XLPRA2 after disease onset, and while photoreceptor cell death was ongoing [at 5 wk, cell death is ∼50% of the maximal rate determined by TUNEL labeling (22)], arrested progression of the disease, and the morphology of the remaining photoreceptors was restored to normal. At least for the stages of disease studied, this therapeutic vector was highly effective and warrants further studies for translational applications. In both models, treatment with the *hIRPB-hRPGR* therapeutic vector prevented (XLPRA1) or reversed (XLPRA2) rod and R/G cone opsin mislocalization, a feature of the disease in human (34), mouse (17), and dog (22, 35) and a putative early marker of photoreceptor cell death (58, 59).

A characteristic feature of photoreceptor degenerations is progressive changes in the OPL, bipolar cells, and inner retinal layers (22, 35–37). These were widespread in untreated areas, but reversed to normal in treated areas, particularly when the *AAV2/5-hIRPB-hRPGR* vector was used. Prevention of remodeling occurred when XLPRA1 retinas were treated before disease onset, whereas, in XLPRA2, early OPL synaptic changes, bipolar cell abnormalities, and inner retinal abnormalities were abrogated with treatment, and normal structure ensued. Thus, treatment of the primary photoreceptor defect has beneficial downstream effects as OPL and inner retinal abnormalities are prevented or reversed. This may account for the improved postreceptoral responses recorded from three of the four treated dogs. Future studies should extend the posttreatment follow-up period to older ages when degeneration of untreated regions would allow testing of treatment consequences at the visual brain such as with the use of pupillometry and visual evoked potentials, and ultimately with visual behavior.

Subretinal treatment in XLPRA canine models of *RPGR*ORF15-XLRP with AAV2/5 vectors and the full-length human *RPGR*ORF15 cDNA was effective in preserving photoreceptor structure and function. The treatment was more effective when the hIRBP promoter regulated the therapeutic transgene rather than the hGRK1 promoter; however, we acknowledge that a much larger sample size is necessary to make a definitive conclusion. The success of this therapeutic approach emphasizes the need for further development of this therapy and paves the way for treating the *RPGR* form of human retinitis pigmentosa.

Materials and Methods

Patients with XLRP and molecularly confirmed *RPGR*ORF15 mutations were included in this study for retinal cross-sectional imaging. XLPRA1 and XLPRA2 dogs were subretinally injected with an AAV2/5 vector carrying a full-length human *RPGR*ORF15 cDNA under the control of either a human IRBP or GRK1 promoter. Assessment of the response to gene transfer was made by means of clinical ophthalmic examinations, *en face* and cross-

sectional in vivo retinal imaging, electroretinography, and morphological evaluation on retinal histological sections. Methodological details are provided in *SI Materials and Methods*.

1. Wright AF, Chakarova CF, Abd El-Aziz MM, Bhattacharya SS (2010) Photoreceptor degeneration: Genetic and mechanistic dissection of a complex trait. *Nat Rev Genet* 11:273–284.
2. Bramall AN, Wright AF, Jacobson SG, McInnes RR (2010) The genomic, biochemical, and cellular responses of the retina in inherited photoreceptor degenerations and prospects for the treatment of these disorders. *Annu Rev Neurosci* 33:441–472.
3. Acland GM, et al. (2001) Gene therapy restores vision in a canine model of childhood blindness. *Nat Genet* 28:92–95.
4. Cideciyan AV (2010) Leber congenital amaurosis due to RPE65 mutations and its treatment with gene therapy. *Prog Retin Eye Res* 29:398–427.
5. Bird AC (1975) X-linked retinitis pigmentosa. *Br J Ophthalmol* 59:177–199.
6. Bhattacharya SS, et al. (1984) Close genetic linkage between X-linked retinitis pigmentosa and a restriction fragment length polymorphism identified by recombinant DNA probe L1.28. *Nature* 309:253–255.
7. Meindl A, et al. (1996) A gene (RPGR) with homology to the RCC1 guanine nucleotide exchange factor is mutated in X-linked retinitis pigmentosa (RP3). *Nat Genet* 13:35–42.
8. Schwahn U, et al. (1998) Positional cloning of the gene for X-linked retinitis pigmentosa 2. *Nat Genet* 19:327–332.
9. Bader I, et al. (2003) X-linked retinitis pigmentosa: *RPGR* mutations in most families with definite X linkage and clustering of mutations in a short sequence stretch of exon ORF15. *Invest Ophthalmol Vis Sci* 44:1458–1463.
10. Sharon D, et al. (2003) RP2 and RPGR mutations and clinical correlations in patients with X-linked retinitis pigmentosa. *Am J Hum Genet* 73:1131–1146.
11. Pelletier V, et al. (2007) Comprehensive survey of mutations in RP2 and RPGR in patients affected with distinct retinal dystrophies: Genotype-phenotype correlations and impact on genetic counseling. *Hum Mutat* 28:81–91.
12. Vervoort R, et al. (2000) Mutational hot spot within a new RPGR exon in X-linked retinitis pigmentosa. *Nat Genet* 25:462–466.
13. Breuer DK, et al. (2002) A comprehensive mutation analysis of RP2 and RPGR in a North American cohort of families with X-linked retinitis pigmentosa. *Am J Hum Genet* 70:1545–1554.
14. Jacobson SG, et al. (1997) Disease expression in X-linked retinitis pigmentosa caused by a putative null mutation in the RPGR gene. *Invest Ophthalmol Vis Sci* 38:1983–1997.
15. Sandberg MA, Rosner B, Weigel-DiFranco C, Dryja TP, Berson EL (2007) Disease course of patients with X-linked retinitis pigmentosa due to RPGR gene mutations. *Invest Ophthalmol Vis Sci* 48:1298–1304.
16. Aleman TS, et al. (2007) Inner retinal abnormalities in X-linked retinitis pigmentosa with RPGR mutations. *Invest Ophthalmol Vis Sci* 48:4759–4765.
17. Hong DH, et al. (2000) A retinitis pigmentosa GTPase regulator (RPGR)-deficient mouse model for X-linked retinitis pigmentosa (RP3). *Proc Natl Acad Sci USA* 97:3649–3654.
18. Chang B, et al. (2002) Retinal degeneration mutants in the mouse. *Vision Res* 42:517–525.
19. Hong DH, Pawlyk BS, Adamian M, Li T (2004) Dominant, gain-of-function mutant produced by truncation of RPGR. *Invest Ophthalmol Vis Sci* 45:36–41.
20. Zhang Q, et al. (2002) Different RPGR exon ORF15 mutations in Canids provide insights into photoreceptor cell degeneration. *Hum Mol Genet* 11:993–1003.
21. Zeiss CJ, Acland GM, Aguirre GD (1999) Retinal pathology of canine X-linked progressive retinal atrophy, the locus homologue of RP3. *Invest Ophthalmol Vis Sci* 40:3292–3304.
22. Beltran WA, Hammond P, Acland GM, Aguirre GD (2006) A frameshift mutation in RPGR exon ORF15 causes photoreceptor degeneration and inner retina remodeling in a model of X-linked retinitis pigmentosa. *Invest Ophthalmol Vis Sci* 47:1669–1681.
23. Wright AF, et al. (2004) Lifespan and mitochondrial control of neurodegeneration. *Nat Genet* 36:1153–1158.
24. Jacobson SG, et al. (2011) Human retinal disease from AIPL1 gene mutations: Foveal cone loss with minimal macular photoreceptors and rod function remaining. *Invest Ophthalmol Vis Sci* 52:70–79.
25. Ayyagari R, et al. (2002) X-linked recessive atrophic macular degeneration from RPGR mutation. *Genomics* 80:166–171.
26. Ebenezer ND, et al. (2005) Identification of novel RPGR ORF15 mutations in X-linked progressive cone-rod dystrophy (XLCORD) families. *Invest Ophthalmol Vis Sci* 46:1891–1898.
27. Shu X, et al. (2007) RPGR mutation analysis and disease: An update. *Hum Mutat* 28:322–328.
28. Walia S, et al. (2008) Discordant phenotypes in fraternal twins having an identical mutation in exon ORF15 of the RPGR gene. *Arch Ophthalmol* 126:379–384.
29. Ruddle JB, et al. (2009) RPGR ORF15 genotype and clinical variability of retinal degeneration in an Australian population. *Br J Ophthalmol* 93:1151–1154.
30. Fahim AT, et al. (2011) Allelic heterogeneity and genetic modifier loci contribute to clinical variation in males with X-linked retinitis pigmentosa due to RPGR mutations. *PLoS ONE* 6:e23021.
31. Mowat FM, et al. (2008) Topographical characterization of cone photoreceptors and the area centralis of the canine retina. *Mol Vis* 14:2518–2527.
32. Acland GM, et al. (2005) Long-term restoration of rod and cone vision by single dose rAAV-mediated gene transfer to the retina in a canine model of childhood blindness. *Mol Ther* 12:1072–1082.
33. Khanna H, et al. (2005) RPGR-ORF15, which is mutated in retinitis pigmentosa, associates with SMC1, SMC3, and microtubule transport proteins. *J Biol Chem* 280:33580–33587.
34. Adamian M, Pawlyk BS, Hong DH, Berson EL (2006) Rod and cone opsin mislocalization in an autopsy eye from a carrier of X-linked retinitis pigmentosa with a Gly436Asp mutation in the RPGR gene. *Am J Ophthalmol* 142:515–518.
35. Beltran WA, Acland GM, Aguirre GD (2009) Age-dependent disease expression determines remodeling of the retinal mosaic in carriers of RPGR exon ORF15 mutations. *Invest Ophthalmol Vis Sci* 50:3985–3995.
36. Aguirre GD, et al. (2002) Retinal histopathology of an XLRP carrier with a mutation in the RPGR exon ORF15. *Exp Eye Res* 75:431–443.
37. Li ZY, Kljavin IJ, Milam AH (1995) Rod photoreceptor neurite sprouting in retinitis pigmentosa. *J Neurosci* 15:5429–5438.
38. Geiger K, et al. (1994) Transgenic mice expressing IFN-gamma in the retina develop inflammation of the eye and photoreceptor loss. *Invest Ophthalmol Vis Sci* 35:2667–2681.
39. Jacobson SG, Cideciyan AV (2010) Treatment possibilities for retinitis pigmentosa. *N Engl J Med* 363:1669–1671.
40. Wright AF, Shu X (2007) Focus on Molecules: RPGR. *Exp Eye Res* 85:1–2.
41. Simons DL, Boye SL, Hauswirth WW, Wu SM (2011) Gene therapy prevents photoreceptor death and preserves retinal function in a Bardet-Biedl syndrome mouse model. *Proc Natl Acad Sci USA* 108:6276–6281.
42. Guyon R, Pearce-Kelling SE, Zeiss CJ, Acland GM, Aguirre GD (2007) Analysis of six candidate genes as potential modifiers of disease expression in canine XLPRA1, a model for human X-linked retinitis pigmentosa 3. *Mol Vis* 13:1094–1105.
43. Demirci FY, et al. (2002) X-linked cone-rod dystrophy (locus COD1): Identification of mutations in RPGR exon ORF15. *Am J Hum Genet* 70:1049–1053.
44. Yang Z, et al. (2002) Mutations in the RPGR gene cause X-linked cone dystrophy. *Hum Mol Genet* 11:605–611.
45. Demirci FY, et al. (2005) Histopathologic study of X-linked cone-rod dystrophy (CORDX1) caused by a mutation in the RPGR exon ORF15. *Am J Ophthalmol* 139:386–388.
46. Alexander JJ, et al. (2007) Restoration of cone vision in a mouse model of achromatopsia. *Nat Med* 13:685–687.
47. Komáromy AM, et al. (2010) Gene therapy rescues cone function in congenital achromatopsia. *Hum Mol Genet* 19:2581–2593.
48. Michalakis S, et al. (2010) Restoration of cone vision in the CNGA3-/- mouse model of congenital complete lack of cone photoreceptor function. *Mol Ther* 18:2057–2063.
49. Carvalho LS, et al. (2011) Long-term and age-dependent restoration of visual function in a mouse model of CNGB3-associated achromatopsia following gene therapy. *Hum Mol Genet* 20:3161–3175.
50. Jacobson SG, et al. (2012) Gene therapy for Leber congenital amaurosis caused by RPE65 mutations: Safety and efficacy in 15 children and adults followed up to 3 years. *Arch Ophthalmol* 130:9–24.
51. Petrs-Silva H, et al. (2011) Novel properties of tyrosine-mutant AAV2 vectors in the mouse retina. *Mol Ther* 19:293–301.
52. He S, et al. (2008) Retinitis pigmentosa GTPase regulator (RPGR) protein isoforms in mammalian retina: Insights into X-linked retinitis pigmentosa and associated ciliopathies. *Vision Res* 48:366–376.
53. Murga-Zamalloa CA, Desai NJ, Hildebrandt F, Khanna H (2010) Interaction of ciliary disease protein retinitis pigmentosa GTPase regulator with nephronophthisis-associated proteins in mammalian retinas. *Mol Vis* 16:1373–1381.
54. Shu X, et al. (2005) RPGR ORF15 isoform co-localizes with RPGRIP1 at centrioles and basal bodies and interacts with nucleophosmin. *Hum Mol Genet* 14:1183–1197.
55. Murga-Zamalloa CA, Atkins SJ, Peranen J, Swaroop A, Khanna H (2010) Interaction of retinitis pigmentosa GTPase regulator (RPGR) with RAB8A GTPase: Implications for cilia dysfunction and photoreceptor degeneration. *Hum Mol Genet* 19:3591–3598.
56. Ghosh AK, et al. (2010) Human retinopathy-associated ciliary protein retinitis pigmentosa GTPase regulator mediates cilia-dependent vertebrate development. *Hum Mol Genet* 19:90–98.
57. Porrello K, Bhat SP, Bok D (1991) Detection of interphotoreceptor retinoid binding protein (IRBP) mRNA in human and cone-dominant squirrel retinas by in situ hybridization. *J Histochem Cytochem* 39:171–176.
58. Alfinito PD, Townes-Anderson E (2002) Activation of mislocalized opsin kills rod cells: A novel mechanism for rod cell death in retinal disease. *Proc Natl Acad Sci USA* 99:5655–5660.
59. Zhang T, Zhang N, Baehr W, Fu Y (2011) Cone opsin determines the time course of cone photoreceptor degeneration in Leber congenital amaurosis. *Proc Natl Acad Sci USA* 108:8879–8884.

NEUROSCIENCE

Beltran et al.